Protein Science (1999), *8*:2773–2783. Cambridge University Press. Printed in the USA.

Synthesis, folding, and structure of the β-turn mimic modified B1 domain of streptococcal protein G

BENOIT ODAERT,[1] FABIENNE JEAN,[1] CHRISTOPHE BOUTILLON,[1,2] ERIC BUISINE,[1,2] OLEG MELNYK,[1] ANDRE TARTAR,[1] AND GUY LIPPENS[1]

[1]Laboratoire Synthèse, Structure, Fonction des Biomolécules UMR 8525, Institut de Biologie de Lille, Institut Pasteur de Lille, 1 rue du Professeur Calmette, BP 447 59021 Lille Cedex, France
[2]Faculté des sciences pharmaceutiques et biologiques, Université de Lille II, 3 rue du Professeur Laguesse, BP83-59006 Lille Cedex, France

(RECEIVED March 29, 1999; ACCEPTED August 11, 1999)

Abstract

The mechanism of β-sheet formation remains a fundamental issue in our understanding of the protein folding process, but is hampered by the often encountered kinetic competition between folding and aggregation. The role of local versus nonlocal interactions has been probed traditionally by mutagenesis of both turn and strand residues. Recently, rigid organic molecules that impose a correct chain reversal have been introduced in several small peptides to isolate the importance of the long-range interactions. Here, we present the incorporation of a well-studied β-turn mimic, designated as the dibenzofuran-based (DBF) amino acid, in the B1 domain of streptococcal protein G (B1G), and compare our results with those obtained upon insertion of the same mimic into the N-terminal β-hairpin of B1G (O Melnyk et al., 1998, *Lett Pept Sci 5*:147–150). The DBF-B1G domain conserves the structure and the functional and thermodynamical properties of the native protein, whereas the modified peptide does not adopt a native-like conformation. The nature of the DBF flanking residues in the modified B1G domain prevents the β-turn mimic from acting as a strong β-sheet nucleator, which reinforces the idea that the native β-hairpin formation is not driven by the β-turn formation, but by tertiary interactions.

Keywords: activity; β-turn mimic; dibenzofuran; domain B1 of protein G; folding; protein engineering; stability; structure

Understanding how a protein folds into its native form still remains a question of fundamental interest for the de novo design of proteins. Peptide studies on α-helix derived fragments support the framework model, with secondary structure elements formed during the initiation of the protein folding process (Dyson et al., 1988; Freund et al., 1996), and have laid the basis for the estimation of α-helix propensity of various peptides (Muñoz & Serrano, 1994a, 1994b). The detailed understanding of β-sheet formation, however, has lagged behind, due to problems in generating soluble β-sheet models that do not aggregate at the concentrations typically used for structural studies. Present studies have essentially been limited to β-hairpins, where the two antiparallel strands are connected by a β-turn (Blanco et al., 1994a; de Alba et al., 1996; Neira & Fersht, 1996; Ramírez-Alvarado et al., 1997). A stable β-turn is thought to act on β-sheet formation as a nucleator or initiation site, from which the two strands apart come closer to each other residue by residue (de Alba et al., 1997; Muñoz et al., 1997; Ramírez-Alvarado et al., 1997; Sheinerman & Brooks, 1998). The combined knowledge of these studies has only very recently led to two soluble mini-proteins that adopt a stable β-sheet in solution (Kortemme et al., 1998; Schenck & Gellman, 1998).

To impose a suitable chain reversal and a correct hydrogen bonding pattern of the directly attached amino acids allowing the formation of the first stabilizing hydrogen bond of the β-sheet, a myriad of synthetic β-turn mimics have been designed and evaluated on their capacity to nucleate β-sheets in small peptides (Baca et al., 1993; Kemp & Li, 1995; Nesloney & Kelly, 1996a, 1996b). One example is the dibenzofuran-based β-turn mimic (Fig. 1B) designed by Díaz and Kelly (1991) that has been thoroughly characterized and successfully incorporated into several small peptides (Díaz et al., 1992, 1993a, 1993b; Tsang et al., 1994).

We recently have set out to incorporate this β-sheet nucleator into a real protein environment as defined by the existence of a full tertiary structure. Scyllatoxin, a 31 amino acid scorpion toxin with

Reprint requests to: G. Lippens, Laboratoire Synthèse, Structure, Fonction des Biomolécules CNRS UMR 8525, Institut de Biologie de Lille, Institut Pasteur de Lille, 1 rue du Professeur Calmette, BP 447 59021 Lille Cedex, France; e-mail: guy.lippens@pasteur-lille.fr.

Abbreviations: 1D, 2D, 3D, one-, two-, and three-dimensional; B1G, B1 domain of the streptococcal protein G; B1G-DBF, DBF-modified B1 domain of the streptococcal protein G; *t*-Boc, *tert*-butyloxycarbonyl; CD, circular dichroism; DBF, dibenzofuran; Gdn·Cl, guanidium hydrochloride; LED, Longitudinal Eddy current Delay; NOE, nuclear Overhauser effect; NOESY, two-dimensional NOE spectroscopy; RP-HPLC, reversed-phase high-performance liquid chromatography; TMSP, trimethylsilyl propionate; TOCSY, two-dimensional total correlation spectroscopy.

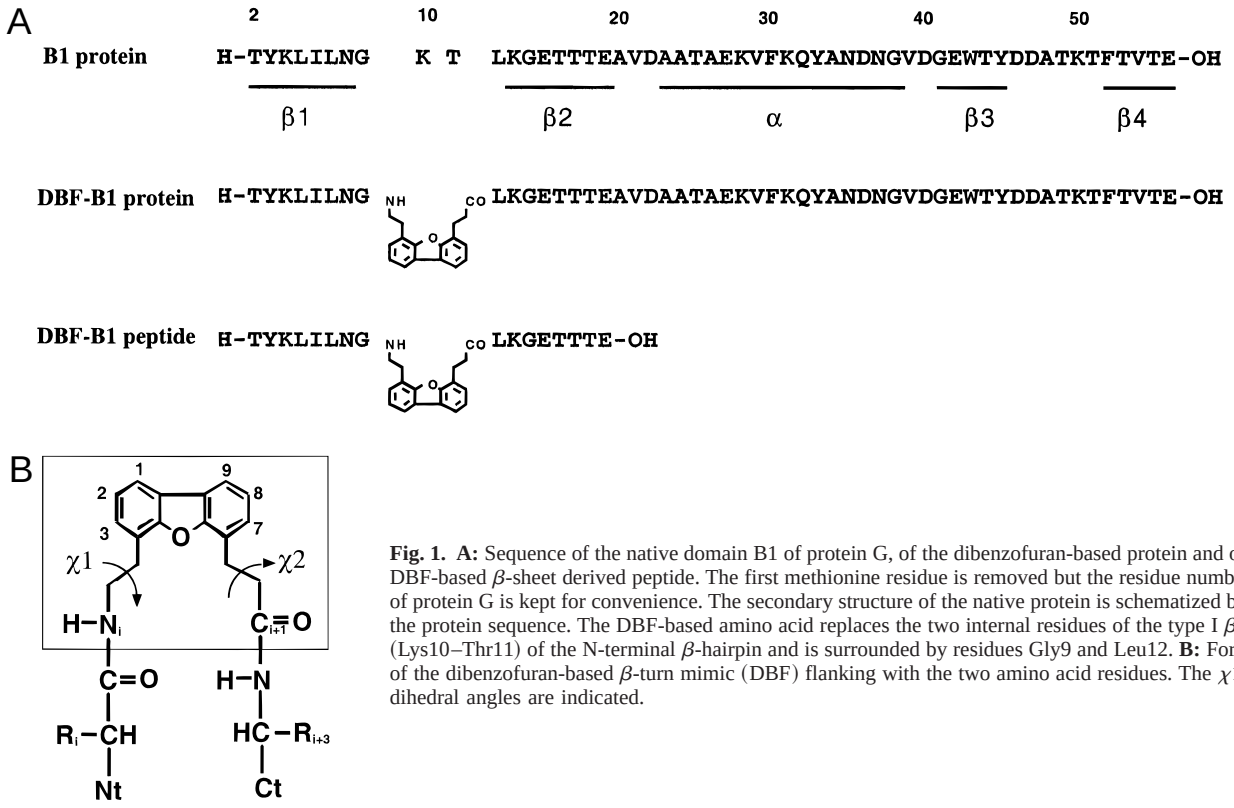

Fig. 1. A: Sequence of the native domain B1 of protein G, of the dibenzofuran-based protein and of the DBF-based β-sheet derived peptide. The first methionine residue is removed but the residue numbering of protein G is kept for convenience. The secondary structure of the native protein is schematized below the protein sequence. The DBF-based amino acid replaces the two internal residues of the type I β-turn (Lys10–Thr11) of the N-terminal β-hairpin and is surrounded by residues Gly9 and Leu12. **B:** Formula of the dibenzofuran-based β-turn mimic (DBF) flanking with the two amino acid residues. The $\chi 1$, $\chi 2$ dihedral angles are indicated.

a disulfide bridge stabilized α/β scaffold (Martins et al., 1995), obeyed our initial constraints placed upon the protein model, as were (1) a small size compatible with peptide synthesis and NMR analysis, (2) the presence of the major secondary structure elements folded into a stable tertiary structure, (3) a solvent exposed β-turn, and (4) an easily detectable biological activity dependent upon the integrity of the structural organization of the protein but not directly involving the amino acids present in the β-turn. The chemical synthesis and refolding of the modified protein were successful, proving that the DBF mimic is compatible with a full protein structure (Jean et al., 1998). However, the presence of three disulfide bridges, crucial for the stability of scyllatoxin, seriously hampered our next objective, which was to evaluate its ability to stabilize the resulting protein.

We therefore turned our attention to a second protein model, devoid of such factors as proline residues, disulfide bridges, or cofactors, that can influence potentially the folding and stability of the molecule. A model of choice is the B1 domain of the streptococcal protein G (B1G), a 56 amino acid protein with a high thermal stability (87 °C at neutral pH) over a wide pH range (2–11). The structure, composed of a four-stranded β-sheet, on top of which lies a long α-helix, has been extensively used for structure and folding studies, by various spectroscopic techniques (Gronenborn et al., 1991, 1996; Alexander et al., 1992b; Frank et al., 1995), by dissection into peptides (Blanco et al., 1994a, 1994b, 1997; Blanco & Serrano, 1995), and by theoretical approaches as well (Sheinerman & Brooks, 1997, 1998). From those studies, a consensus model has arisen, with initial formation of the C-terminal β-hairpin, consequent formation of the α-helix and final formation of the compact native state. Of particular interest is the high flexibility of the isolated N-terminal fragment of B1G in aqueous solution (Blanco et al., 1994a), with two local low populated chain bends involving residues 8–9 and 14–15, a structure that is different from the final folded state of that region in the protein. Our first effort to enforce a correct chain bending by inserting in the N-terminal fragment the DBF-based mimic at the position of the native type I β-turn motif failed, because the hydrophobic nature of the mimic led to various non-native contacts and probably to aggregation (Melnyk et al., 1998). The present study, therefore, was aimed at answering two questions: (1) can the cooperativity of the protein folding process overcome the problems encountered upon insertion of the mimic in the N-terminal peptide, and (2) can we evaluate the extent to which the mimic stabilizes or not the B1G domain?

We have synthesized the B1G domain with a DBF-based mimic replacing the residues 10 and 11, and report here our results on the synthesis and folding of the resulting molecule. The conformational properties of the DBF-B1G molecule have been examined by CD and ^{1}H-NMR. The modified protein adopts the native protein conformation, but is locally affected by the mimic insertion. Comparison with the native and the modified N-terminal peptides reinforces the idea that tertiary interactions constitute the driving forces of the folding of the B1 domain of the streptococcal protein G.

Results

Synthesis

Despite its more important size, the synthesis of DBF-B1G was more efficient than that of the DBF-scyllatoxin (Jean et al., 1998).

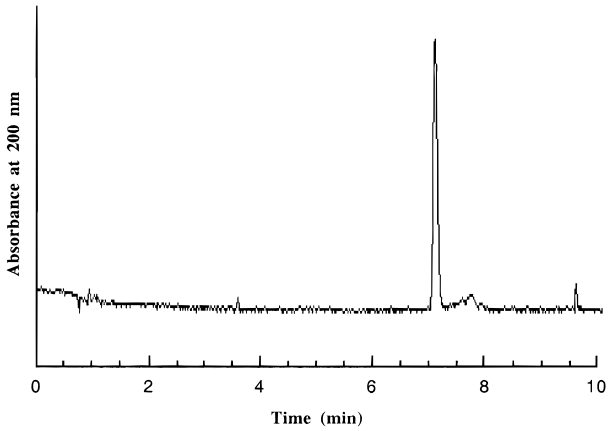

Fig. 2. Capillary zone electrophoresis profile of the B1G-DBF molecule after preparative RP-HPLC and ion-exchange HPLC.

The yield of chain assembly for the modified protein (30%) is slightly lower than for the native protein (36%), while for the modified scyllatoxin (25%) it was severely reduced compared to the native yield (60%). The hydrophobic and rigid nature of the DBF moiety is probably responsible for the decrease of the accessibility of the reactive amine function to the active ester, thereby reducing the coupling efficiency. The success of the DBF-B1G synthesis over the DBF-scyllatoxin's is related to the location of the modified β-turn in the peptidic sequence. In contrast to scyllatoxin, the modified β-turn in B1G is close to the N-terminal end and, therefore, incorporation of DBF affects only the last steps of the solid phase peptide synthesis.

The crude product of the synthesis dissolved in 6 M Gdn·Cl was analyzed by RP-HPLC. The major peak has the expected deconvoluted molecular mass of 6,100.0 Da. The purification process involved slow dialysis against water, preparative HPLC on CN and C18 columns, and finally, a step of ion exchange chromatography (Fig. 2). The purified peptide was analyzed by RP-HPLC, capillary electrophoresis, electrospray mass spectroscopy, and amino acid analysis. Five milligrams of the purified product after desalting were obtained for the functional and structural characterization by CD and NMR spectroscopies.

Monomeric state

To test the possibility of aggregation or oligomer formation, line widths measured on a high-resolution 1D spectrum, chemical shift variations as measured in 2D TOCSY experiments and translational self-diffusion coefficients measured with the pulsed field-gradient LED sequence (Altieri et al., 1995) were monitored as a function of protein concentration. At 298 K and pH 3.3, these parameters remained essentially constant between 1.2 and 0.1 mM. At this latter concentration, the diffusion coefficient of the DBF-B1G protein was only 9% slower than that of the native synthetic protein (1.41×10^{-10} m^2 s^{-1} for the B1 domain and 1.30×10^{-10} m^2 s^{-1} for the B1G-DBF molecule). CD measurements at concentrations between 120 and 1.5 μM did show only marginal differences (data not shown), and, more importantly, the wavelength of maximal absorbance (280 nm) of all aromatic signals, with a major contribution of the DBF aromatic ring (17,797 mol^{-1} cm^{-1}, compared to 10,030 mol^{-1} cm^{-1} for the B1 domain) did not shift over the whole concentration range. All these arguments support the view that the DBF-B1G molecule is monomeric under the conditions used for the structural analysis.

Circular dichroism

The native B1G and DBF-B1G molecules display very similar far-ultraviolet (UV) CD spectra with a well-defined minimum at 208 nm and a maximum at 192 nm (Fig. 3). This spectral identity supports the view of the conservation of the overall secondary structure of the latter, despite the mimic incorporation. An absorption band at 255 nm in the absorption spectrum was observed for the modified protein, resulting from the successful incorporation of the DBF moiety. Moreover, the observation of a slight positive ellipticity (150 deg cm^2 $dmol^{-1}$), previously assigned to the formation of a cluster between the dibenzofuran moiety and the hydrophobic side chains of the flanking residues (Tsang et al., 1994), indicates that the dibenzofuran is in an asymmetric environment. However, the signal of the near-UV is sevenfold less intense than those observed in various DBF-peptide models, suggesting that this hydrophobic cluster is not well defined.

^{1}H-NMR assignment

Standard two-dimensional sequence-specific methods (Wüthrich, 1986) lead to a quasi-complete assignment of the ^{1}H-NMR spectra of the DBF-B1G. Linebroadening was observed for the resonances of the residues immediately flanking the mimic and prevented assignment of the L12 and K13 residues resonances. Chemical shifts of the proton resonances at 288 and 298 K are given in Supplementary material in Electronic Appendix.

Conservation of the native protein structure

To check the influence of the DBF insertion on the folding of the peptidic part of the modified protein, we compared our NMR parameters to the structural data obtained on the native B1G domain (Gronenborn et al., 1991). The majority of backbone proton chemical shifts did not differ by more than 0.1 ppm (Fig. 4), indicating an identical 3D environment. The same equivalence was

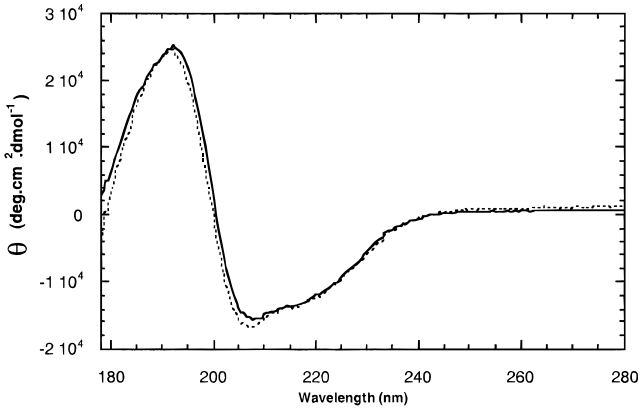

Fig. 3. CD analysis of the native protein G (—) and of the DBF-modified protein G (- - -). Sample conditions: 0.1 mM protein concentration, pH 3.2, 291 K in water.

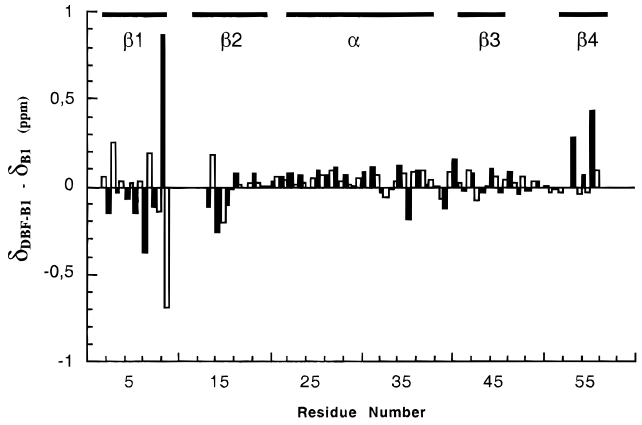

Fig. 4. Amide (■) and Hα (□) protons backbone chemical shift differences along the amino acid sequence, using the native B1 domain of protein G as a reference (Gronenborn et al., 1991). The gap in the profile corresponds to the two internal β-turn residues Lys10 and Thr11 replaced by the DBF-based amino acid, and by the unassigned Leu12 and Lys13 residues.

also observed for the majority of side-chain resonances. We examined in a second phase the NOE network to compare the secondary and tertiary structure of the native and modified proteins. The extended conformation of the four native β-strands (Gronenborn et al., 1991; Gallagher et al., 1994) was readily identified in the DBF-B1G molecule on the basis of the characteristic pattern of sequential backbone NOEs (Table 1), and their correct pairing into a four-stranded β-sheet was verified by the Hα-Hα contacts between residues of the different strands (Fig. 5). The central fragment 22–37 adopts a regular α-helical conformation, based on the continuous $NN(i, i + 1)$ NOEs and on the presence of medium intensity $\alpha\beta(i, i + 3)$ and weak intensity $\alpha N(i, i + 3)$ connectivities (Table 1). In the native B1G domain, the residues between positions 46 and 51 connecting the two segments β3 and β4 adopt an unusual six residue β-turn. The same irregular turn region was identified in the DBF-B1G molecule, based on the simultaneous presence of strong intensity $NN(i, i + 1)$ contacts in this region and medium intensity αN(46,48) and αN(48,50) cross peaks.

The compact hydrophobic core of the native protein gives rise to a dense network of NOE contacts between aromatic and aliphatic side-chain protons (Gronenborn et al., 1991), and the same contacts were observable in the DBF-B1G molecule (Fig. 6A,B). It should be noted that Tyr3, Leu5, Leu7 residues on the β1 strand and Thr16 and Thr18 residues on the β2 strand, despite their presence on the modified hairpin, have their side chain directed to the interior of the molecule and participate to the hydrophobic core. We, therefore, concluded that the DBF insertion does not noticeably disturb the hydrophobic core of the protein, which was shown to be one of the early events in the folding (Kuszewski et al., 1994; Park et al., 1997; Sheinerman & Brooks, 1998) and one of the crucial elements of the protein stability (O'Neil et al., 1995; Gronenborn et al., 1996).

We finally performed amide exchange experiments to verify the conservation of the native hydrogen bonds, which are equally essential for the stability of the native B1G domain. Whereas the pattern of protected amide protons, as monitored by their presence after 12 and 36 h of exchange, is close to that of the native B1G domain (Fig. 5) (Orban et al., 1994, 1995), the region around the DBF, and noticeably the amide protons of Gln42 and Glu56, exchange faster than in the native B1G domain.

To further assess the conservation of the native overall structure, binding to Fc and Fab fragments of IgG (Erntell et al., 1988) was evaluated by a competitive ELISA test applied previously on the

Table 1. *Sequential backbone NOE connectivities* [a]

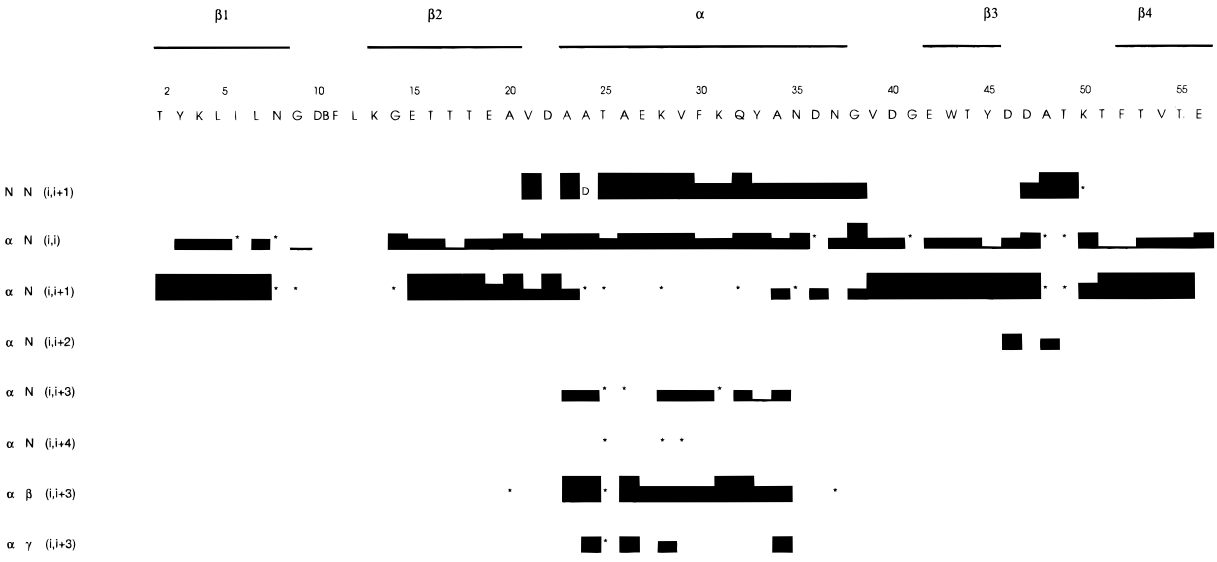

[a]Derived from the 300 ms mixing time NOESY spectrum acquired at 288 K, pH 3.3 in H_2O. Intensity of NOE cross peaks is proportionally indicated by the height of each box. Overlapping is indicated either with an asterisk or with the diagonal (D).

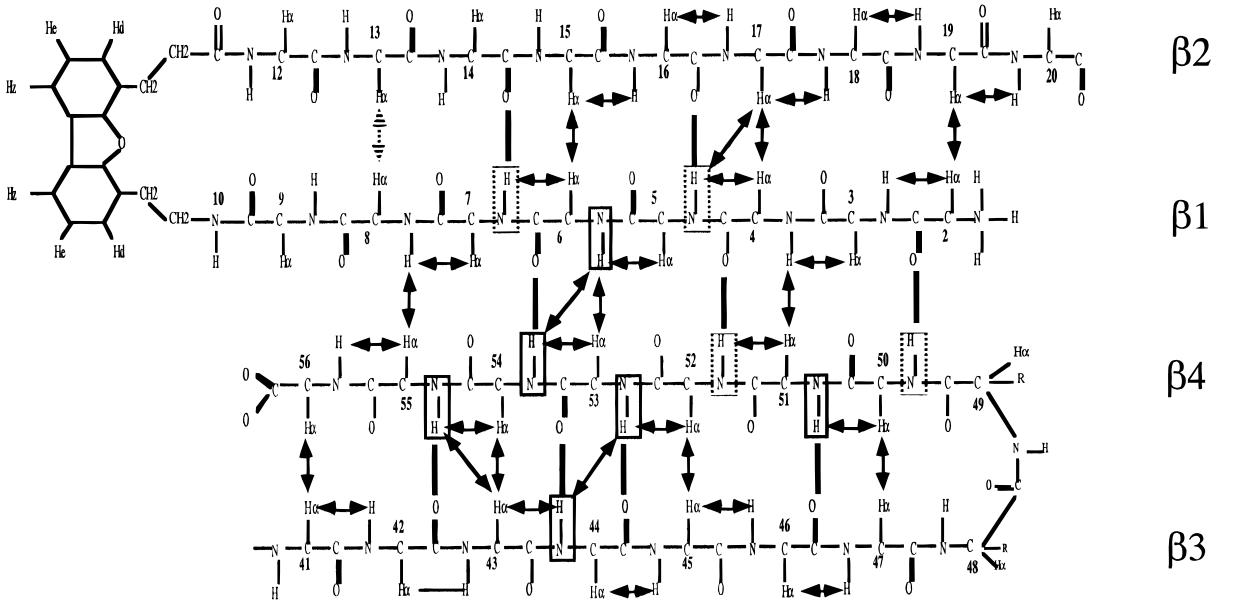

Fig. 5. Schematic representation of the sequential and tertiary backbone connectivities and of the exchange protected amide protons supporting the formation of the native four-stranded β-sheet. NOE connectivities are displayed by arrows. The dashed arrow recalls the ambiguity of the αα(8,13) connectivity. Highly protected amide protons (still observed in the 36 h) are distinguished from weakly protected amide protons (exchanged after 12 h) by straight lined boxes.

synthetic B1G domain (Boutillon et al., 1995). The modified protein retains its ability to bind each fragment with high affinity in comparison to the native one.

Local effect of the mimic on the protein structure

In the modified protein, the two strands β1 and β2 surrounding the mimic form the native antiparallel β-sheet (vide supra). However, in the direct environment of the mimic, line broadening affects all resonances from residues Ile6 or Glu15 to the mimic flanking residues Gly9 and Leu12, respectively. We attribute this very localized line broadening probably to a conformational exchange process at the intermediate time scale (Huang & Oas, 1995; Kaplan, 1996), where the chemical shift values are modulated by the varying ring current effect of the moving DBF aromatic moiety, which is in a flexible but not totally disordered state. If we extrapolate to the DBF-B1G molecule, the chemical shift variations Δω observed upon insertion of the DBF mimic into scyllatoxin (Jean et al., 1998), and use the quadratic dependence of the line broadening on Δω, the exchange process can be estimated to occur on the millisecond time scale.

Based on the NMR results, it is clear that the influence of the mimic extends beyond the modified β-sheet central residues. Chemical shift deviations of more than 0.1 ppm were observed in the central part of the modified β-sheet, but also at the protein C-terminus (residues 54 to 56) and in the loop region at the C-terminus of the α-helix (residues Val39 and Gln42).

Molecular modeling of the DBF-B1G domain

A molecular model of the DBF-B1G molecule was generated by inserting the lowest energy conformation of the DBF moiety into the B1G structure. Because the overall protein structure remains conserved despite the insertion of the DBF, only the conformation of a well-defined subset of residues in the spatial vicinity of the mimic (Asn8, Gly9, Leu12, Lys13, Glu56, and the stretch from residues 34 to 40) was exhaustively explored through a torsional angle driving procedure.

The dihedral angles χ1 and χ2 around the two ethyl groups branched at the DBF N- and C-termini, describing completely the mimic conformation, were systematically varied, and low-energy conformations after a minimization step were recorded. The lowest energy regions correspond to a well-defined fork of χ2 angles around 70°, but differ in the χ1 angle value (Fig 7). They correspond only to conformations where the DBF is folded onto the side chains of Gly9 and Leu12 (Fig. 8), and hence, located on the inner face of the β-sheet, relatively close to the side chains of Val39 and Glu56 residues. When averaged over the allowed χ1 values, we equally observed a weakening of the first hydrogen bond after the turn.

In the modified scyllatoxin, the two mimic flanking residues, Ile22 and Lys25, both have long aliphatic side chains and form a hydrophobic cluster with the dibenzofuran aromatic ring (Jean et al., 1998). The absence of side chain in the DBF-B1G molecule at one DBF-flanking position is probably the reason for the observed flexibility by NMR spectroscopy. To test this hypothesis, we mutated in the DBF-B1G model the flanking glycine by an isoleucine, whose bulky aliphatic side chain can favor the cluster formation. The molecule DBF-B1G(I,L)^{MU} was then subjected to the previously described torsion angle driving procedure. The resulting energy landscape along the χ1 and χ2 now displays unique well-defined energy well, as observed for the DBF-modified scyllatoxin. Whereas the DBF moiety in the mutant polypeptide is still folded toward the inner face of the β-sheet, the hydrophobic interaction fixes the flanking residues such as to adopt the native β-turn hydrogen bond, and changes significantly the (χ1, χ2)

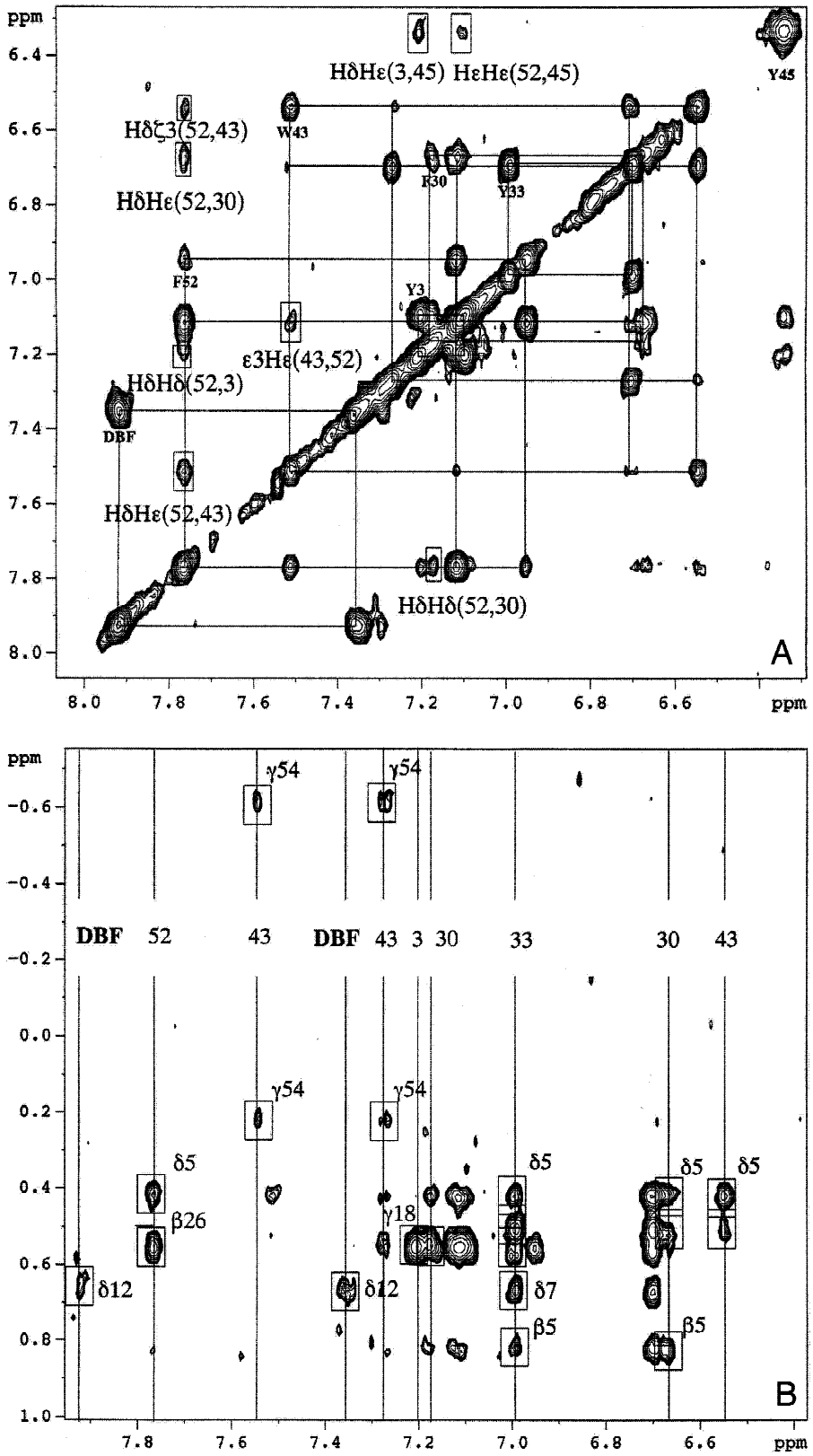

Fig. 6. A: Aromatic–aromatic proton region of a 300 ms NOESY spectrum acquired at 288 K, pH 3.3 in D_2O. Networks of intraresidue resonances of aromatic ring protons are displayed by straight lines. Annotated boxes indicate the tertiary NOE connectivities between aromatic side chain protons. **B:** Aromatic–aliphatic proton region of a 300 ms NOESY spectrum acquired at 288 K, pH 3.3 in D_2O. Straight lines along the F1 dimension indicate the nonoverlapped aromatic side-chain proton resonances. NOE cross peaks with aliphatic residue protons are boxed and assigned. The observed NOE connectivities with the DBF aromatic protons could arise with the δCH3 protons of the unassigned Leu12 or with the γCH3 protons of Val39.

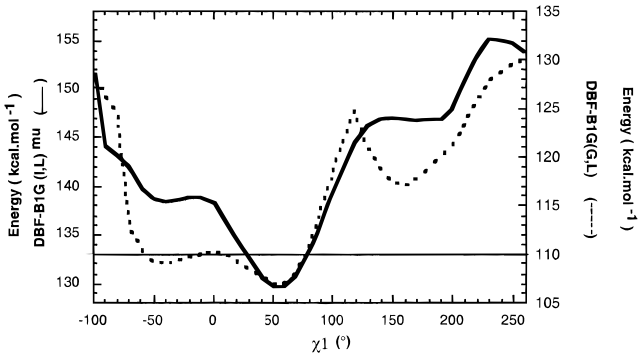

Fig. 7. Energy profile vs. the $\chi 1$ angle for DBF-B1G(G,L) (- - -) and isoleucine mutant DBF-B1G(I,L)^{MU} (—). For both B1G and DBF-B1G molecules, the $\chi 2$ value of $-70°$ corresponds to the minimal energy along the $\chi 2$ axis.

profile. Although the $\chi 2$ value for the lowest energy conformations is not changed by the mutation, the $\chi 1$ value is now restricted around 60° (Fig. 7), as it was observed upon incorporation of the DBF moiety in scyllatoxin. It confirms that removing the side-chain interactions with the aromatic moiety is at the basis of the increased flexibility at the DBF N-terminus.

Thermal and pH stability of B1G and DBF-B1G domains

To test the effect of the DBF insertion on protein stability, the pH and thermal denaturation curves of native and modified protein were recorded by far-UV CD spectroscopy. No major change was observed in the far-UV region upon varying the pH from 1 to 10 (data not shown), indicating that the modified protein remains folded at room temperature over a wide range of pH, similar to the native protein (Goward et al., 1991). The sigmoidal character of the thermal denaturation curve shows the high cooperativity of the unfolding process for both synthetic B1G and DBF-B1G domains (Fig. 9). Thermodynamic parameters were extracted by a fitting procedure (see Materials and methods), assuming a ΔC_p value of 2.6 kJ/mol K^{-1} as previously determined on the B1G domain (Alexander et al., 1992a). Compared to the synthetic B1G domain, the modified protein seems to be slightly less thermostable with a 3 K decrease in the T_m (Table 2). This difference can be considered as significant, because the observed T_m during unfolding and refolding differed by less than 1 K. The resulting value of $\Delta\Delta G_0$ (1.3 kJ/mol) at the T_m is three times weaker than the reported values for the disruption of a single hydrogen bond (Koh et al., 1997), suggesting that the DBF insertion has a little effect on the protein stability at room temperature. [It should be noted that the synthetic B1G domain is significantly less stable than the recombinant protein studied at the same pH (T_m = 353 K, $\Delta G_{278\ K}$ = 28 kJ/

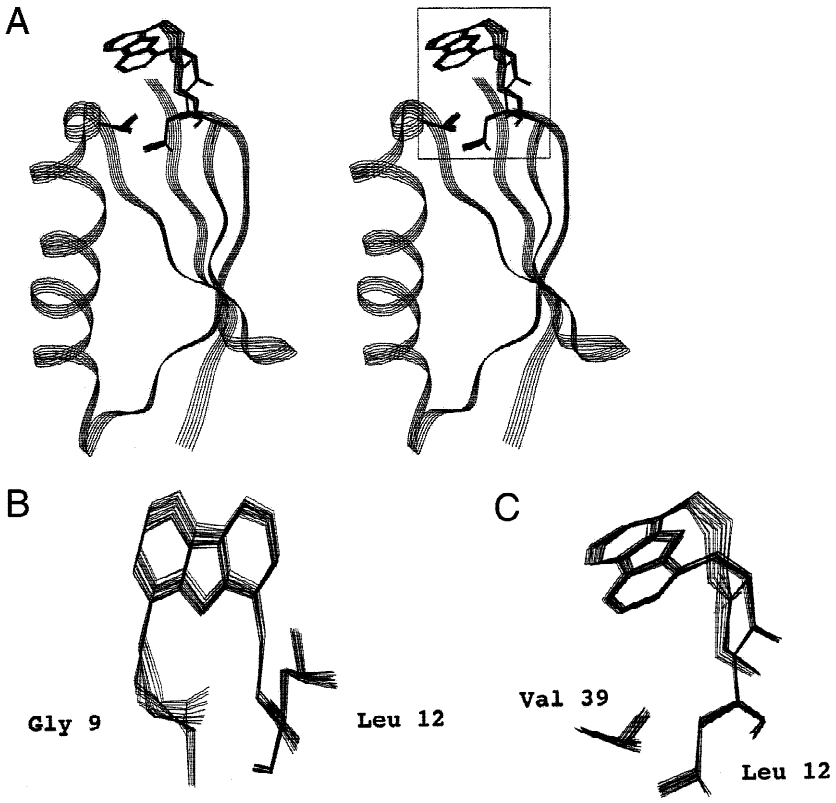

Fig. 8. A: Stereoview of the 21 minimum energy conformers of the DBF-B1G molecule obtained with the torsion angle driving procedure. The conformers are superimposed with respect to the backbone atoms of the B1G domain drawn in gray. **B,C:** Detailed view of the mimic region showing the hydrophobic cluster between the aromatic moiety with the aliphatic side chains of the flanking Leu12 and the spatially adjacent Val39 residues. Note the flexibility at the N-terminal extremity of the mimic around the Gly9 residue. **C:** Detailed view of the mimic region showing the hydrophobic cluster between the aromatic moiety with the aliphatic side chains of the flanking Leu12 and the spatially adjacent Val39 residues. Note the flexibility at the N-terminal extremity of the mimic around the Gly9 residue.

Table 2. *Thermodynamic data for synthetic B1G and DBF-B1G molecules* [a]

	T_m (K)	ΔH_m (kJ/mol)	ΔS_m (J/mol K)	ΔG 278 K (kJ/mol)
B1G	327.9 ± 0.1	159.8 ± 3.4	487 ± 10	13.9 ± 0.5
DBF-B1G	325.2 ± 0.2	157.7 ± 4.3	485 ± 13	13.5 ± 0.6

[a] Thermal denaturations were done at pH 3.5 in 50 mM sodium acetate. The ΔC_p value (2.6 kJ K^{-1} mol^{-1}) determined for the recombinant B1G domain (1) was used in the fitting procedure by assuming no change upon mutation.

mol). In fact, the recombinant protein kept its N-terminal methionine and has been shown to be substantially more stable even at the optimal pH (by around 7 kJ/mol at pH 5.4) than the 55-residue protein (Minor & Kim, 1994a). Moreover, the melting transition temperature of the B1G domain is known to decrease rapidly below pH 4.0 due to the increasing positive charge of the protein. So the combination of these two factors can explain the apparent discrepancy between our results and the literature.]

Discussion

The engineering of stable, folded, and functional polypeptides has attracted a lot of research attention (Dalal et al., 1997; Rose, 1997; Hellinga, 1998; Malakauskas & Mayo, 1998), both from the fundamental side of understanding the interactions that govern folding, and from the applied side, to increase stability or alter function of the resulting molecules. Recently, the notion of a kinetic competition between productive folding and aggregation (Fink, 1998) has entered the field, and understanding the factors that dominate this competition will be of considerable interest to intervene in the aggregation process. β-Sheet model systems, in contrast to α-helical peptides, are particularly prone to aggregation, and only very recently have two research groups succeeded to produce a soluble mini-protein that adopts a stable β-sheet in solution (Kortemme et al., 1998; Schenck & Gellman, 1998). Whereas this opens the possibility to study the different factors that govern the secondary structure element formation, it will not be easy to separate the influence of the turn residues from the interactions across the two strands.

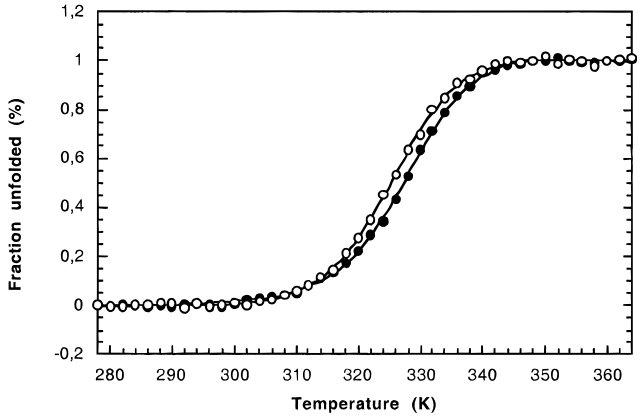

Fig. 9. Equilibrium unfolding of the native B1G (●) and DBF-B1G (○) domains in 50 mM sodium acetate buffer at pH 3.5 as monitored by the change of the ellipticity value at 218 nm. The experimental points are represented as symbols, and the line represents the nonlinear least-squares best fit to a two-state model.

Whereas the field has traditionally relied on mutagenesis techniques, a different approach is the merging of chemistry and biology by coupling of peptide fragments to produce larger objects (Muir et al., 1998; Severinov & Muir, 1998) or by inserting non-natural amino acids during the chemical synthesis of the peptide. Organic chemistry has delivered numerous rigid organic building blocks that enforce a correct chain bending and, in the best of cases, allow formation of the first interstrand hydrogen bond, and a large number of them has been tested in small peptide models (Díaz & Kelly, 1991; Baca et al., 1993; Kemp & Li, 1995). However, besides the continuing problems with aggregation, it is still unclear to what extent these small model peptides are representative for full protein structures, characterized by a well-defined tertiary structure. Our laboratory has therefore set out to study the influence of incorporation into different protein models of one particular mimic, based on the dibenzofuran aromatic system (Díaz & Kelly, 1991). Despite the hydrophobic nature of the latter, our first attempt successfully led to the DBF-syllatoxin molecule, which maintained the native fold and function (Jean et al., 1998) but showed a faster kinetics of disulfide reduction with concomitant unfolding. Because the disulfide bridges are the major factor determining the stability of scyllatoxin, we decided to introduce the mimic in a second protein model, the B1 domain of streptococcal protein G, devoid of such factors as disulfide bridges, proline residues or cofactors, that all might influence its stability.

Evidence for the overall structure conservation of the DBF-B1G domain came from its ability to bind correctly the Fc and Fab fragments of the IgG antibody, and by the nearly identical NMR parameters (chemical shift values, NOE pattern, and protection factors) for the native and modified B1 domains, except for some protons in the direct spatial environment of the DBF moiety. The situation there is significantly different for the modified scyllatoxin and B1G proteins. In the former, the DBF ring stacked tightly onto the outward pointing aliphatic side chains of the flanking residues I22 and K25, isolating the aromatic ring from the rest of the protein. The mimic proved compatible with the geometry of the native turn region, and no change in twist of the β-hairpin was observed (Jean et al., 1998). In the modified B1 domain, the mimic is flanked by the residues G9 and L12, located on the inner face of the N-terminal β-hairpin. The absence of a side chain for Gly9 prohibits any well-defined interactions with the flanking residues and induces a significant degree of flexibility, as suggested by the local line broadening. Our modeling studies on the mutant proteins, DBF-B1G(I,L)^{MU}, offers some insight into this phenomenon: the absence of close hydrophobic contacts with the flanking aliphatic side chains leads to a wider valley of low-energy states, allowing a conformational freedom for the aromatic moiety. The absence of a hydrophobic cluster between the DBF ring and the N-terminal flanking Gly9 is probably compensated by a tertiary interaction with the aliphatic side chain of the V39 residue, resulting in an interaction between the DBF moiety and both the β4 strand and the loop at the C-terminus of the α helix. This proximity is supported both by changes in the proton chemical shift values and by our molecular modeling. Finally, the significant changes of several amide and Hα proton chemical shift values corresponding to residues in the β1 strand might not be explained only by the ring current effect of the DBF moiety, but could well correspond to

subtle conformational changes of the protein backbone. The geometry of the mimetic in this precise turn is probably not optimal, prevents formation of the first hydrogen bond of the native β-turn, and therefore introduces conformational flexibility on the first β-strand. However, these conformational changes are not sufficient to prevent the correct folding of the modified protein, and, as demonstrated by thermal and pH denaturation studies, have only a weak influence on the stability of the DBF-B1G domain that is only slightly less stable than the native protein.

The isolated N-terminal hairpin-derived peptide of the native B1G is very flexible in solution, with only some evidence for a chain reversal at residues 7 and 10 when 30% TFE is added to the aqueous solution (Blanco et al., 1994a). This flexibility, together with the displacement of the turn region by one residue compared to the native conformation in the protein, suggests that in this precise case, the native β-turn is not a dominant factor in the early events of the β-sheet formation, although more generally, there is ample evidence that the β-turn region does play an important role (de Alba et al., 1996; Ramírez-Alvarado et al., 1997). Our preliminary attempt to nucleate the formation of the β-hairpin in the isolated peptide failed, because of the presence of a glycine residue flanking the mimic at its N-terminal side (Melnyk et al., 1998), in agreement with the absolute requirement of a hydrophobic cluster or π cation-like interactions with the side chains of the flanking residues in order for the mimic to nucleate the β-sheet (Graciani et al., 1994; Tsang et al., 1994). The absence of a side chain on the glycine residue at the DBF flanking position led to several nonnative contacts between the aromatic moiety and the side chains of Leu7 and/or Leu5, and the hydrophobic nature of this cluster was the probable source of aggregation.

The same Leu side chains in the modified B1G protein have at first sight two choices: they could make hydrophobic contacts with the mimic, as in the isolated peptide, or complete the hydrophobic core, as observed in the native protein. Our results of a correctly folded and stable DBF-B1G protein lead to the conclusion that in this case the hydrophobic core formation is the most efficient pathway, both from a kinetic and thermodynamical point of view. This has several important implications for our understanding of protein folding. First, it corroborates the recent proposal of an early intermediate in the folding reaction of the B1G domain, containing a native-like core but excluding the N-terminal tail (Park et al., 1997), which was presented as an argument against a folding mechanism involving a random hydrophobic collapse. Second, it is in agreement with the proposed cooperativity of the folding process of β-sheets (Muñoz et al., 1997; Schenck & Gellman, 1998). More precisely, the suggested initial formation of the C-terminal β-hairpin folding, providing a template on which the N-terminal secondary structure element can fold, is confirmed by the hydrophobic core competing successfully for the side-chain interactions of the different leucine side chains on the first strand. Although the nature of the flanking residues was not suitable for the mimic to nucleate the β-hairpin formation, the DBF-B1G domain retains the native fold, proving that nonlocal interactions can dominate the folding of such complex molecules as are proteins. However, even though the correct fold of the DBF-B1 domain underlines the importance of nonlocal interactions (Minor & Kim, 1994b), it is necessarily preceded by the correct assembly in a hydrophobic core of the side chains coming from other parts of the molecule, notably the C-terminal hairpin and the α-helix. Therefore, our study is equally in agreement with the framework model, where local interactions in the very early steps of protein folding lead to the formation of native like secondary structure elements that further guide the assembly into near-native conformational states by a correct side-chain packing (Dyson et al., 1988; Dobson et al., 1994). Protein engineering allows modification of those local interactions: their enhancement at the solvent-exposed sites in native α-helices has increased the speed of folding and the resulting stability (Villegas et al., 1995; Muñoz et al., 1996; Viguera et al., 1996), whereas introducing non-native local interactions was shown to destabilize the protein rather than alter the correct folding (Prieto et al., 1997). However, recently it has become clear that aggregation potentially can compete with the folding process (Radford & Dobson, 1999; Fink, 1998) and therefore limits the modifications that one can introduce.

We can conclude that our study is in agreement with the overall folding picture of the B1 domain, with early formation of the C-terminal β-hairpin and α-helix, whose side chains form the hydrophobic core that successfully competes with the DBF moiety for the aliphatic side chains on the N-terminal β-hairpin. Whereas the competition between aggregation and folding in this case is tipped to the latter, it is clear that to be successful in protein engineering, more hydrophilic mimics will have to be developed.

Materials and methods

Synthesis and purification of DBF-B1G

The DBF-based β-turn mimic (Fig. 1B) was synthesized according to the method published by Kelly (Díaz & Kelly, 1991). The peptide chain of DBF-GB1 (Fig. 1A) was synthesized using a *t*-Boc/benzyl strategy (Merrifield, 1986), with a *t*-Boc-Glu(OBzl) OCH_2phenyl acetamidomethyl resin (Applied Biosystems, Foster City, California). *t*-Boc protected amino acids (Novabiochem, Läufelfingen, Switzerland) had the following side-chain protections: benzyl (Bzl) for Ser and Thr, trityl (Trt) for Asn and Gln, cyclohexyl (cHx) for Asp and Glu, 2-chlorobenzyloxycarbonyl (2ClZ) for Lys, and 2-bromobenzyloxycarbonyl for Tyr. Before the incorporation of the DBF β-turn mimic (Glu56 to Leu12), the synthesis was achieved on a ABI 430 peptide synthesizer (Applied Biosystems) according to a previously optimized protocole (Boutillon et al., 1995), with double or triple couplings, depending on coupling difficulties. The β-turn mimic was incorporated manually. The coupling procedure was as follows. The first coupling was performed with 3 eq. DBF-mimic(Boc), 2.7 eq. HBTU/HOBt, 9 eq. DIEA in 2 mL DMF for 1 h, the second and third couplings with 2 eq. DBF-mimic(Boc) for 50 min, 1.8 eq. HBTU/HOBt, 6 eq. DIEA in 2 mL DMF for 1 h. After the incorporation of the DBF-mimic, triple couplings were achieved manually, using BOP for the third coupling. On completion of the synthesis, DBF-B1G was deprotected and removed from the resin with HF in the presence of the usual scavengers (*p*-cresol, *p*-thiocresol) and dibenzofuran.

The crude product was dissolved in 6 M guanidinium hydrochloride, 0.1 M Na_2HPO_4 buffer pH 5.7, purified by preparative RP-HPLC on a CN column and then on a C18 column. The product was finally purifed by preparative anion-exchange chromatography (Gel Q Sepharose-Pharmacia) and then desalted by RP-HPLC and analyzed by capillary zone electrophoresis on a 50 cm long capillary using a buffer solution of 20 mM sodium citrate, pH 2.5, at 30 °C. Mass spectroscopy by electrospray gave satisfactory results (Obsd: 6,100.0 ± 0.3 Da; calcd for $C_{275}H_{410}N_{64}O_{93}$ (isotopic average): 6,100.7 Da).

Circular dichroism

Far-UV CD spectra were recorded on a Jobin-Yvon (Longjuneau, France) CD6 instrument calibrated with (1S)-(+)-10-camphorsulfonic acid. Comparative spectra for native B1G and DBF-B1G samples were recorded from 178 to 280 nm on a cell with optical path length of 0.1 mm by taking every 0.5 nm with a 30 s integration time and a 2 nm slit width. Sample conditions were 18 °C, pH 3.2 without salt, and protein concentrations of 0.1 mM as determined by amino acid analysis. pH stability was tested by adjusting the pH between 1 and 11, as obtained by adding small amounts of concentrated HCl or NaOH. Thermal denaturations were done on 10 μM protein solutions with a 1 cm path length cell at pH 3.5 in the presence of 50 mM sodium acetate. The temperature was raised from 5 to 91 °C every 2 °C, with a stabilization delay of 5 min and a precision of 0.05 °C. The reverse process allowed testing of the reversibility of the denaturation. The CD signal was acquired at 218 nm, with an integration time of 1 min as was previously done for the native B1G domain (O'Neil et al., 1995). The melting curves were fitted to a two-state model after pre- and post-transitional slope correction by using the Gibbs–Helmholtz equation for the unfolding free energy

$$\Delta G = \Delta H_m - T\Delta S_m + \Delta C_p\,(T - T_m - T\ln(T/T_m)) = -RT\ln([U]/[F]) \quad (1)$$

where ΔH_m and ΔS_m are the enthalpy and entropy of unfolding evaluated at the melting temperature, ΔG the free energy of unfolding at the temperature T, $[F]$ and $[U]$ the concentrations of the folded and unfolded states at the temperature T (O'Neil et al., 1995).

^{1}H-NMR spectroscopy

Experiments were performed on a Bruker DMX 600 MHz spectrometer and processed with the Bruker software. The DBF-B1G molecule was dissolved in 90% H_2O/10% D_2O solution (pH 3.2) or 100% D_2O to get a final concentration of 0.1 mM. TOCSY and NOESY spectra were acquired at 288 and 298 K with mixing times, respectively, of 50, 100 ms and of 150, 300 ms. 2D spectra were acquired with 256 complex points in F1 dimension and 2,048 points in F2 dimension. Amide exchange studies were done by solubilizing the protonated lyophilized protein in pure D_2O. For the exchange studies, a series of NOESY spectra were acquired with a time resolution of about 12 h. Translational diffusion coefficients (Ds) were measured with the pulsed field-gradient LED sequence (Altieri et al., 1995) in which a WET sequence was incorporated for water suppression.

Molecular modeling

Molecular modeling calculations were performed on a Silicon Graphic workstation with the Insight II and Discover modules of the Biosym_msi software (Biosym, San Diego, California). The CVFF force field was used for energy minimization.

A hybrid molecule was generated by merging the lowest energy mimic conformations and the B1G protein coordinates (entry name 1GB1 in the Brookhaven Protein Data Bank) in a similar way as for scyllatoxin (Jean et al., 1998). To explore the conformational space accessible to the mimic, the $\chi 1$ and $\chi 2$ dihedral angles around the two ethyl arms flanking the DBF moiety at its respective N- and C-terminus (Fig. 1B) were subjected to a torsional angle driving, with systematic 10° increments. Outside of a radius of 7 Å centered on the oxygen of the furan entity, the rest of the molecule was kept fixed. An energy minimization procedure with a 0.1 kcal/mol Å^{-1} threshold for the energy gradient was applied at every step of the torsional angle driving.

In a second phase, the DBF-B1G molecule was modified by the mutation Gly → Ile. The wild-type hybrid designated as B1G(G,L) for DBF-B1G was mutated in B1G(I,L)^{MU}. The first letter in bracket refer to the mutable residue preceding the mimic and the second letter to the conserved residue following the mimic. The mutant was subjected to the above described procedure for wild-type hybrids.

Geometric analysis was done on conformations comprised within a fork of 3 kcal/mol from the lowest energy conformation.

Supplementary material in Electronic Appendix

Tables of 1H chemical shifts at pH 3.2 and 288 K (filename: CS_288K) and at 298 K (filename:CS_298K) (Microsoft Word Version 6.0.1 for Power MacIntosh).

Acknowledgments

We thank J.-M. Wieruszeski and G. Montagne for excellent assistance with the NMR and CD experiments, D. Horvath for his help in molecular modelling, H. Drobecq for his help in protein purification, and L. Vallard for tests in binding essays. The 600 MHz facility used in this study was funded by the European Community (FEDER), the Région Nord–Pas de Calais (France), the CNRS, and the Institut Pasteur de Lille. Part of this work was financed by EU Grant BIO4-CT97-2086.

References

Alexander P, Fahnestock S, Lee T, Orban J, Bryan P. 1992a. Thermodynamic analysis of the folding of the streptococcal protein G IgG-binding domains B1 and B2: Why small proteins tend to have high denaturation temperatures? *Biochemistry 31*:3597–3603.

Alexander P, Orban J, Bryan P. 1992b. Kinetic analysis of folding and unfolding the 56 amino acid IgG-binding domain of streptococcal protein G. *Biochemistry 31*:7243–7248.

Altieri AS, Hinton DP, Byrd RA. 1995. Association of biomolecular systems *via* pulsed field gradient NMR self-diffusion measurements. *J Am Chem Soc 117*:7566–7567.

Baca M, Alewood PF, Kent SBH. 1993. Structural engineering of the HIV-1 protease molecule with a β-turn of fixed geometry. *Protein Sci 2*:1085–1091.

Blanco FJ, Jiménez MA, Pienda A, Rico M, Santoro J, Nieto JL. 1994a. NMR solution structure of the isolated fragment of the N-terminal fragment of protein-G B1 domain. Evidence of trifluoroethanol induced native-like β-hairpin formation. *Biochemistry 33*:6004–6014.

Blanco FJ, Ortiz AR, Serrano L. 1997. Role of a nonnative interaction in the folding of the protein G B1 domain as inferred from the conformational analysis of the α-helix fragment. *Folding Design 2*:123–133.

Blanco FJ, Rivas G, Serrano L. 1994b. A short linear peptide that folds into a native stable β-hairpin in aqueous solution. *Struct Biol 1*:584–590.

Blanco FJ, Serrano L. 1995. Folding of protein G B1 domain studied by the conformational characterization of fragments comprising its secondary structure elements. *Eur J Biochem 230*:634–649.

Boutillon C, Wintjens R, Lippens G, Drobecq H, Tartar A. 1995. Synthesis, three-dimensional structure, and specific ^{15}N labelling of the streptococcal protein G B1-domain. *Eur J Biochem 231*:166–180.

Dalal S, Balasubramanian S, Regan L. 1997. Protein alchemy: Changing β-sheet into α-helix. *Nat Struct Biol 4*:548–552.

de Alba E, Jiménez MA, Rico M. 1997. Turn residue sequence determines β-hairpin conformation in design peptides. *J Am Chem Soc 119*:175–183.

de Alba E, Jiménez MA, Rica M, Nieto JL. 1996. Conformational investigation of designed short linear peptides able to fold into β-hairpin structures in aqueous solution. *Folding Design 1*:133–144.

Díaz H, Espina JR, Kelly JW. 1992. A dibenzofuran-based amino acid designed to nucleate antiparallel β-sheet structure: Evidence for intramolecular hydrogen-bond formation. *J Am Chem Soc 114*:8316–8318.

Díaz H, Kelly JW. 1991. The synthesis of dibenzofuran based diacids and amino acids designed to nucleate parallel and antiparallel β-sheet formation. *Tetrahedron 32*:5725–5728.
Díaz H, Tsang KD, Choo D, Kelly JW. 1993a. The design of water soluble β-sheet structure based on a nucleation strategy. *Tetrahedron 49*:3533–3545.
Díaz H, Tsang KY, Choo D, Espina JR, Kelly JW. 1993b. Design, synthesis, and partial characterization of water-soluble β-sheets stabilized by a dibenzofuran-based amino acid. *J Am Chem Soc 115*:3790–3791.
Dobson CM, Evans PA, Radford SE. 1994. Understanding how proteins fold. *Trends Biosci 19*:31–37.
Dyson HJ, Rance M, Houghten RA, Wright PE, Lerner RA. 1988. Folding of immunogenic peptide fragments of proteins in water solution. II. The nascent helix. *J Mol Biol 201*:201–217.
Erntell M, Myhre EB, Sjöbring U, Björk L. 1988. Streptococcal protein G has affinity for both Fab- and Fc-fragment of human IgG. *Mol Immun 25*:121–126.
Fink AL. 1998. Protein aggregation: Folding aggregates, inclusion bodies and amyloid. *Folding Design 3*:9–23.
Frank MK, Glore GM, Gronenborn AM. 1995. Structural and dynamic characterization of the urea denatured state of the immunoglobulin binding domain of streptococcal protein G by multidimensional heteronuclear NMR spectroscopy. *Protein Sci 4*:2605–2615.
Freund SMV, Wong K-B, Fehrst AR. 1996. Initiation sites of protein folding by NMR analysis. *Proc Natl Acad Sci USA 93*:10600–10603.
Gallagher T, Alexander P, Bryan P, Gilliland GL. 1994. Two crystal structures of the B1 immunoglobulin-binding domain of streptococcal protein G and comparison with NMR. *Biochemistry 33*:4721–4729.
Goward CR, Irons LI, Murphy JP, Atkinson T. 1991. The secondary structure of protein G, a robust molecule. *Biochem J 274*:503–507.
Graciani NR, Tsang KY, McCutchen SL, Kelly JW. 1994. Amino acids that specify structure through hydrophobic clustering and histidine-aromatic interactions lead to biologically active peptidomimetics. *Bioorg Med Chem 2*:999–1006.
Gronenborn AM, Filpula DR, Essig NZ, Achari A, Whitlow M, Wingfield PT, Clore GM. 1991. A novel, highly stable fold of the immunoglobulin binding domain of streptococcal protein G. *Science 253*:657–661.
Gronenborn AM, Frank K, Clore GM. 1996. Core mutants of the immunoglobulin binding domain of the streptococcal protein G: Stability and structural integrity. *FEBS Lett 398*:312–316.
Hellinga HW. 1998. Computational protein engineering. *Nat Struct Biol 5*:525–527.
Huang GS, Oas TG. 1995. Submillisecond folding of monomeric λ repressor. *Proc Natl Acad Sci USA 92*:6878–6882.
Jean F, Buisine E, Melnyk O, Drobecq H, Odaert B, Hugues M, Lippens G, Tartar A. 1998. Synthesis and structural and functional evaluation of a protein modified with a *b*-turn mimic. *J Am Chem Soc 120*:6076–6083.
Kaplan JI. 1996. Chemical exchange effects on spectra. In: *Encyclopedia of nuclear magnetic resonance*, vol. 2. New York: Wiley. pp 1247–1256.
Kemp DS, Li ZQ. 1995. A short β-sheet containing proline nucleated by a 2,2′-substituted tolan β-turn mimetic. *Tetrahedron Lett 36*:4179–4180.
Koh JT, Cornish VW, Schultz PG. 1997. An experimental approach to evaluating the role of backbone interactions in proteins using unnatural amino acid mutagenesis. *Biochemistry 36*:11314–11322.
Kortemme T, Ramirez-Alvarado M, Serrano L. 1998. Design of a 20-amino acid three-stranded β-sheet protein. *Science 281*:253–256.
Kuszewski J, Clore GM, Gronenborn AM. 1994. Fast folding of a prototypic polypeptide: The immunoglobulin binding domain of streptococcal protein G. *Protein Sci 3*:1945–1952.
Malakauskas SM, Mayo SL. 1998. Design, structure and stability of a hyperthermophilic protein variant. *Nat Struct Biol 5*:470–475.
Martins JC, van de Ven FJM, Borremans FAM. 1995. Determination of the three-dimensional solution structure of scyllatoxin by ^{1}H nuclear magnetic resonance. *J Mol Biol 253*:590–603.
Melnyk O, Boutillon C, Draffan L, Odaert B, Jean F, Lippens G, Tartar A. 1998. Incorporation of a β-turn mimic in the N-terminal fragment of the B1 domain of streptococcal protein G. *Lett Pept Sci 5*:147–150.
Merrifield B. 1986. Solid phase peptide synthesis. *Science 232*:341–347.
Minor DL, Kim PS. 1994a. Measurement of the β-sheet-forming propensities of amino acids. *Nature 367*:660–663.
Minor DL, Kim PS. 1994b. Context is a major determinant of β-sheet propensity. *Nature 371*:264–267.
Muir TW, Sondhi D, Cole PA. 1998. Expressed protein ligation: A general method for protein engineering. *Proc Natl Acad Sci USA 95*:6705–6710.
Muñoz V, Cronet P, López-Hernández E, Serrano L. 1996. Analysis of the effect of local interactions in protein stability. *Folding Design 1*:167–178.
Muñoz V, Serrano L. 1994a. Elucidating the folding problem of α-helical peptides using empirical parameters. *Nat Struct Biol 1*:399–409.
Muñoz V, Serrano L. 1994b. Elucidating the folding problem of α-helical peptides using empirical parameters, II. Helix macrodipole effects and rational modification of the helical content of natural peptides. *J Mol Biol 245*:275–296.
Muñoz V, Thomson PA, Hofrichter J, Eaton WA. 1997. Folding dynamics and mechanism of β-hairpin formation. *Nature 390*:196–199.
Neira JL, Fersht AR. 1996. An NMR study on the β-hairpin region of barnase. *Folding Design 1*:231–241.
Nesloney CL, Kelly JW. 1996a. Progress towards understanding β-sheet structure. *Bioorg Med Chem 4*:739–766.
Nesloney CL, Kelly JW. 1996b. Synthesis and hydrogen bonding capabilities of biphenyl-based amino acids designed to nucleate β-sheet structure. *J Org Chem 61*:3127–3137.
O'Neil KT, Hoess RH, Raleigh DP, DeGrado WF. 1995. Thermodynamic genetics of the folding of the B1 immunoglobulin-binding domain from streptococcal protein G. *Proteins Struct Funct Genet 21*:11–21.
Orban J, Alexander P, Bryan P. 1994. Hydrogen-deuterium exchange in the free and immunoglobulin G-bound protein G B-domain. *Biochemistry 33*:5702–5710.
Orban J, Alexander P, Bryan P, Khare D. 1995. Assessment of stability differences in the protein G B1 and B2 domains from hydrogen–deuterium exchange: Comparison with calorimetric data. *Biochemistry 34*:15291–15300.
Park S, O'Neil KT, Roder H. 1997. An early intermediate in the folding reaction of the B1 domain of protein G contains a native-like Core. *Biochemistry 36*:14277–14283.
Prieto J, Wilmans M, Jiménez MA, Rico M, Serrano L. 1997. Non-native local interactions in protein folding and stability: Introducing a helical tendency in the all β-sheet α-spectrin SH3 domain. *J Mol Biol 268*:760–778.
Radford SE, Dobson CM. 1999. From computer simulations to human disease: Emerging themes in protein. *Cell 97*:291–298.
Ramírez-Alvarado M, Blanco FJ, Niemann, H, Serrano L. 1997. Role of β-turn residues in β-hairpin formation and stability in designed peptides. *J Mol Biol 273*:898–912.
Rose GD. 1997. Protein folding and the Paracelsus challenge. *Nat Struct Biol 4*:512–514.
Schenck HL, Gellman SH. 1998. Use of a designed triple-stranded antiparallel β-sheet to probe β-sheet cooperativity in aqueous solution. *J Am Chem Soc 120*:4869–4870.
Severinov K, Muir TW. 1998. Expressed protein ligation, a novel method for studying protein-protein interactions in transcription. *J Biol Chem 273*:16205–16209.
Sheinerman FB, Brooks CL III. 1997. A molecular dynamics simulation study of segment B1 of protein G. *Proteins Struct Funct Genet 29*:193–202.
Sheinerman FB, Brooks CL III. 1998. Molecular picture of folding of a small α/β protein. *Proc Natl Acad Sci USA 95*:1562–1567.
Tsang KY, Diaz H, Graciani N, Kelly JW. 1994. Hydrophobic cluster formation is necessary for dibenzofuran-based amino acids to function as β-sheeet nucleators. *J Am Chem Soc 116*:3988–4005.
Viguera AR, Villegas V, Avilés FX, Serrano L. 1996. Favourable native-like helical local interactions can accelerate protein folding. *Folding Design 2*:23–33.
Villegas V, Viguera AR, Avilés FX, Serrano L. 1995. Stabilization of proteins by rational design of α-helix stability using helix/coil transition theory. *Folding Design 1*:29–34.
Wüthrich K. 1986. *NMR of proteins and nucleics acids*. New York: Wiley.